ELSEVIER

Journal of Alloys and Compounds 434–435 (2007) 18–21

Journal of ALLOYS AND COMPOUNDS

www.elsevier.com/locate/jallcom

Calorimetric and microstructural analysis of deformation induced crystallization reactions in amorphous $Al_{88}Y_7Fe_5$ alloy

R.J. Hebert [a,*], N. Boucharat [a], J.H. Perepezko [b], H. Rösner [a], G. Wilde [a]

[a] *Chemical, Materials, and Biomolecular Engineering Department, University of Connecticut, Storrs, CT 06269, USA*
[b] *Department of Materials Science and Engineering, University of Wisconsin-Madison, Madison, WI 53706, USA*

Available online 5 December 2006

Abstract

Microcalorimeter and TEM analyses reflect growth of rolling induced Al nanocrystals in shear bands of amorphous $Al_{88}Y_7Fe_5$ alloys at 60 °C as well as a lowering of the crystallization onset temperature of cold rolled samples. Deformation induced Al nanocrystals moreover differ from thermally induced Al nanocrystals in their prolate morphology and the presence of dislocations in some nanocrystals.

Keywords: Amorphous metals; Nanostructures; Liquid quenching; Thermal analysis

1. Introduction

While the crystallization of amorphous alloys during thermal processing has received longstanding attraction [1–3], primary nanocrystals can also develop during intense plastic deformation at room temperature. For Al based amorphous alloys, nanocrystals have first been deformation induced in shear bands of bent ribbons [4], but they have also been detected for ball-milled [5], cold rolled [6], and high pressure torsion strained samples [7]. Attempts to rationalize the deformation induced crystallization reactions have focused on two approaches. In one rationale, it was suggested that adiabatic heating during deformation could raise the temperature in the shear bands sufficiently to induce nanocrystals thermally [8]. The experimental evidence summarized by Jiang and Atzmon [9], however, suggests strongly that the crystallization was a mechanically induced effect. Alternatively, an increase in free volume during deformation would enhance the mobility of atoms in the shear bands sufficiently to induce crystallization even at near ambient temperatures [9,10]. In order to examine the proposed mobility enhancement in shear bands and to compare the morphology and microstructure of the deformation induced and thermally induced Al nanocrystals, rolling and annealing experiments were conducted with amorphous $Al_{88}Y_7Fe_5$ ribbons.

2. Experimental procedures

After arc melting of the $Al_{88}Y_7Fe_5$ master ingot, ribbons were melt-spun in a He-atmosphere at a He pressure of 200 mbar at a wheel-speed of 42 m/s. To characterize the melt-spun ribbons, X-ray diffraction patterns were recorded with a PanAnalytical X'Pert diffractometer using Cu Kα radiation. The samples for transmission electron microscopy (TEM) were electrolytically thinned in a mixture of nitric acid and methanol. A Philips Tecnai F20 ST TEM (operating voltage: 200 kV) was used for the TEM imaging. Thermal analysis was conducted with a Thermometric TAMIII microcalorimeter with micro-Watt sensitivity.

3. Results and discussion

The dark-field (DF) TEM image of the as-spun sample depicted in Fig. 1a demonstrates that within the resolution limit of the TEM imaging, nanocrystals cannot be detected in the as-spun sample. The lower size limit for the detection of nanocrystals is approximately 2 nm. The experience with annealing treatments of the amorphous $Al_{88}Y_7Fe_5$ alloy suggests that during annealing at 210 °C for 10 min, nanocrystals should not develop. Fig. 1a demonstrates that nanocrystals can indeed not be detected in the amorphous phase after the annealing at 210 °C for 10 min. Following cold rolling of the as-spun ribbons to a true strain of approximately −3, nanocrystals can be identified in shear bands and the image in Fig. 1a (lower left) is similar to the DF TEM images of bent Al based amorphous ribbons [4,9]. Following annealing of the cold rolled sample, the nanocrystal density appears to increase (Fig. 1a, lower right image). Moreover, the nanocrystal distribution is more homogeneous than in the cold-

* Corresponding author. Tel.: +1 860 486 3155.
E-mail address: rhebert@ims.uconn.edu (R.J. Hebert).

0925-8388/$ – see front matter © 2006 Published by Elsevier B.V.
doi:10.1016/j.jallcom.2006.08.134

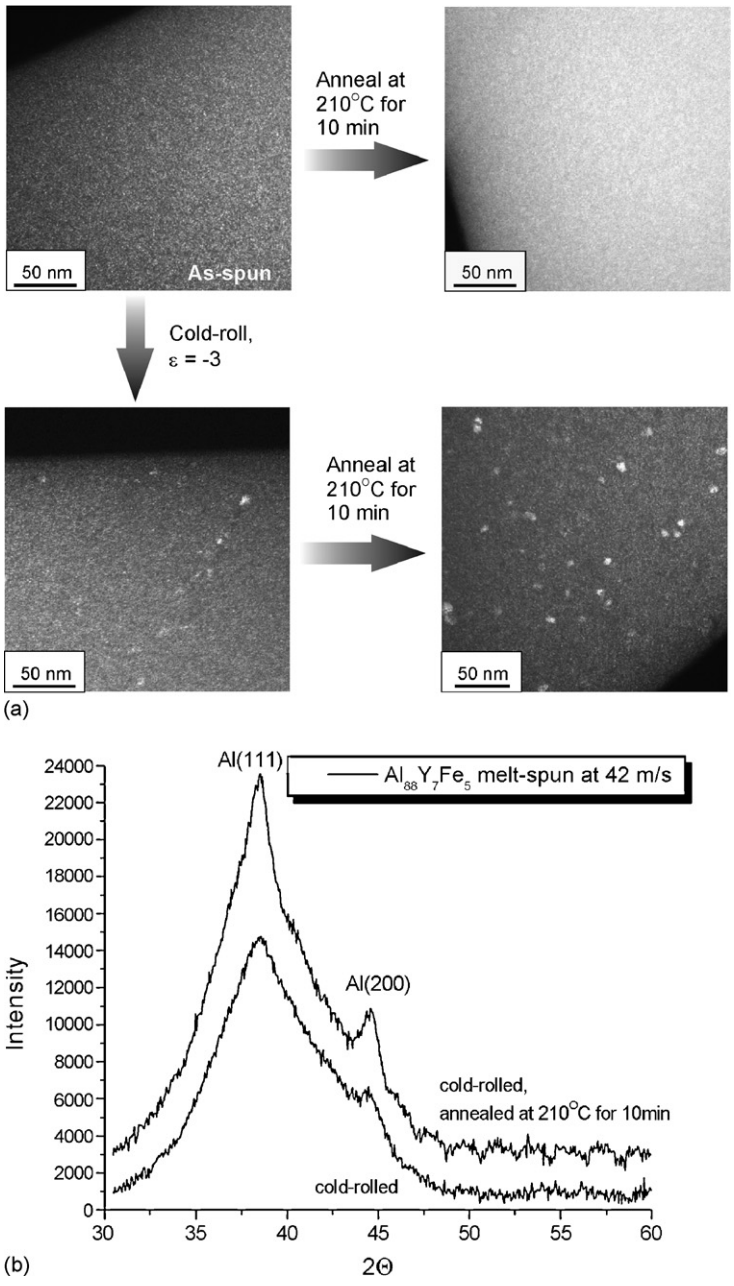

Fig. 1. (a) DF TEM images of as-spun ribbon (upper left image) and of samples after rolling to a true strain of approximately −3 (lower left), annealing at 210 °C for 10 min (upper right), and after rolling and annealing (lower right). (b) X-ray diffraction patterns corresponding to the TEM images of the cold rolled and rolled and annealed samples in (a).

rolled sample, indicating that nanocrystals develop not only in shear bands, but also in the matrix. The increase in the number of nanocrystals observed in the TEM image of the cold rolled and annealed sample could be related to an increased TEM sample foil thickness. The X-ray patterns that are shown in Fig. 1b, however, reveal an increase in the intensity of the Al (2 0 0) peak that is superposed on a broad peak, while an Al (1 1 1) peak has developed in the X-ray pattern of the rolled and annealed sample. The sampling of macroscopic volume fractions during the X-ray diffraction measurement, along with an increase in the Al peak intensities, demonstrates that the increase in the number of Al nanocrystals in the TEM image is due to an increase in the crystallized volume fraction and not due to a thicker TEM foil.

The increase in the fraction of nanocrystalline phase during the annealing of cold rolled samples under annealing conditions that are insufficient to induce observable crystallization for the as-spun ribbon indicates that the rolling induces changes in the amorphous phase that lower the crystallization onset temperature. It has been proposed that the deformation induced crystallization reaction in shear bands resulted from an enhanced free volume in the shear bands that was tantamount to an enhanced mobility of the atoms in the shear bands [4,9,10]. If the enhanced free volume would remain in the shear bands

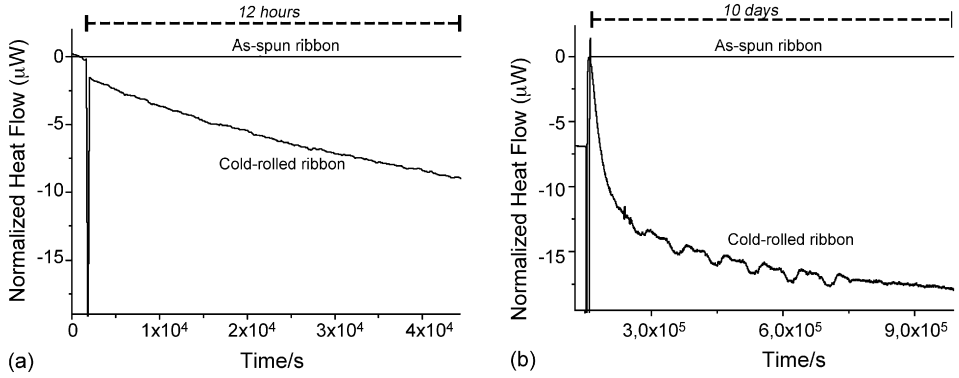

Fig. 2. Isothermal signals of as-spun and cold rolled ribbons at (a) 30 °C and (b) 60 °C.

after deformation, then thermally induced primary crystallization could be expected to occur at temperatures below the onset temperature of the as-spun ribbon. A cold rolled $Al_{88}Y_7Fe_5$ sample was therefore annealed in a microcalorimeter at 60 °C for 10 days. The heating rate from the start temperature of 30 °C to the annealing temperature was 1 K/h. The relative comparison of the isothermal annealing at 30 °C and at 60 °C is depicted in Fig. 2a and b, respectively. The as-spun sample that was annealed under the same conditions as the cold rolled sample (30 °C, 12 h; 60 °C, 10 days) does not reveal any heat release, as the horizontal lines in the diagram demonstrates. By contrast, the cold rolled sample reveals a decaying signal at both annealing temperatures. While the reaction rate (slope of the heat flow curve) is nearly constant at 30 °C within the annealing time, the reaction rate decreases and approaches zero after 10 days of annealing at 60 °C. The pattern in the signal of the cold rolled sample appears to be an artefact and not caused by the sample. A TEM based analysis of the cold rolled and annealed sample at 60 °C demonstrates that unlike for the sample annealed at 210 °C after deformation that revealed a more homogeneous nanocrystal dispersion in the matrix, nanocrystals remain located in the shear bands. The analysis of the particle size distribution for the cold rolled sample and the sample after rolling and annealing that is depicted in Fig. 3 demonstrates that the size distribution has shifted towards bigger particle sizes for the annealed sample. The average particle size increased from 6 to 7 nm. If the growth process would follow a square root dependence ($r \approx \sqrt{Dt}$), the diffusion coefficient would amount to approximately 10^{-24} m^2/s. The annealing at 60 °C for 10 days thus induces a growth of the nanocrystals in the shear bands. The distributions reflect a growth of the average particle size by approximately 1 nm. The data indicates that at the upper end of the size distribution, i.e., at a size of approximately 8–10 nm, the growth seems to be more limited than at the smaller particle sizes. The growth of the biggest nanoparticles could be limited through the width of the shear bands. Once the nanocrystal size approaches the width of the shear band, growth would slow down perpendicular to the shear band boundary because of the reduced mobility in the matrix outside the shear band. Diffusion field impingement within the shear band could act as an additional growth limitation.

The total amount of heat released during the annealing at 60 °C is approximately 2 J/g. The decreasing heat flow during the isothermal annealing suggests that the heat release originated from a growth process and not from a nucleation and growth process [11]. To discern, if a value of 2 J/g would be consistent with a growth of the nanocrystals in the shear bands, it is assumed that all nanocrystals grow from a size of 6 to 7 nm. The values of 6 and 7 nm represent the average sizes of the size distributions of the nanoparticles after rolling and after rolling and annealing, respectively. Taking into account a crystallization enthalpy of -2.84×10^8 J/m^3 [12], the heat released per growing particle would be approximately 1.9×10^{-17} J. The value of -2.84×10^8 J/m^3 has been corroborated for a crystallization temperature of 245 °C. At room temperature, a ΔC_p correction has to be taken into account. Since the temperature dependence of the specific heat in the undercooled regime is not known, a correction of 10% is used to estimate an upper and lower bound of the heat released. A second assumption has to be made regarding the density of the nanocrystals in the shear bands. Over a typical length of the shear bands in the images of approximately 50 nm, one or two deformation induced nanocrystals have typically developed. The width of the shear band is approximately 10–50 nm. The extent of the shear band in the TEM sample in its third dimension cannot

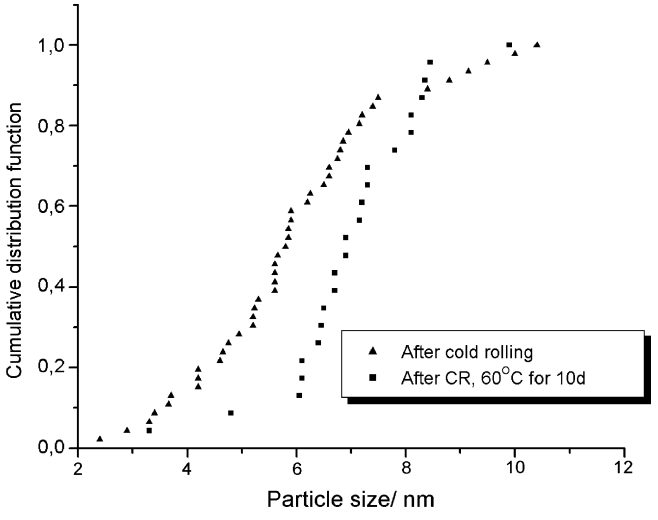

Fig. 3. Particle size distribution of nanocrystals in shear bands after rolling and after rolling and annealing at 60 °C for 10 days.

exceed the foil thickness that is of the order of 100 nm. The particle density of the nanocrystals in the shear band is thus of the order of 4×10^{21} to 8×10^{22} m^{-3}. With a particle density in the shear band of 4×10^{21} to 8×10^{22} m^{-3} and taking into account the estimated ΔC_p correction to the crystallization enthalpy, the heat release upon growth of the nanocrystals in the shear bands would be about 6.8×10^4 to 1.6×10^6 J/m^3 shear band. Taking into account an experimentally determined density of the amorphous alloy of approximately 2.9 g/cm^3, the measured heat release of 2 J/g corresponds to a heat release of about 5.8×10^6 J/m^3. The estimation shows that given the uncertainty in the shear band volume and volume fraction, and the crystallization enthalpy, the growth of the nanocrystals in the shear bands could approximately account for the measured heat release. In addition to the growth of the nanoparticles, relaxation – in particular in shear bands – could serve as a source for the measured heat release. Further studies are necessary to examine the shear band volume and the relaxation behavior of the deformed ribbons.

4. Conclusions

Nanocrystals develop in deformed samples at strain levels of −3 predominantly in shear bands. Combined rolling and annealing studies along with a TEM and microcalorimeter analysis revealed that growth of nanocrystals can take place in shear bands at near ambient temperatures. At the same time, the crystallization in the matrix outside the shear bands at temperatures that are insufficient to induce a noticeable amount of nanocrystals in the as-spun ribbon indicates that the deformation process affects the amorphous phase to promote crystallization below the onset of crystallization of the as-spun sample. Unlike the thermally induced nanocrystals that are defect free and spherical or dendritic, the deformation induced nanocrystals have a tendency for a prolate morphology and some of the deformation induced nanocrystals reveal dislocations. The results suggest that the deformation and annealing at near ambient temperatures alter the arrangement of atoms in the amorphous phase without inducing nanocrystals. Microcalorimetry combined with a statistical analysis of TEM images represents a new experimental strategy to study changes in the amorphous phases due to external forcing (driven conditions) and during relaxation.

Acknowledgements

The help of Mr. T. Scherer for the TEM sample preparation is most gratefully acknowledged. One of the authors (JHP) gratefully acknowledges the award of the Research Center Karlsruhe (320/20260517/INT) and support from the ARO (DAAD 19-02-1-0245).

References

[1] Z.C. Zhong, X.Y. Jiang, A.L. Greer, Philos. Mag. B 76 (1997) 505–510.
[2] J.H. Perepezko, R.J. Hebert, JOM March (2002).
[3] L.Q. Xing, A. Mukopadhyay, W.E. Buhro, K.F. Kelton, Philos. Mag. Lett. 84 (5) (2004) 293–302.
[4] H. Chen, Y. He, G.J. Shiflet, S.J. Poon, Nature 367 (1994) 541–543.
[5] R. Schulz, M.L. Trudeau, D. Dussault, A. Van Neste, Colloque de Physique C4 (1990) C4 259–C4 264.
[6] R.J. Hebert, J.H. Perepezko, Mater. Sci. Eng. A 375–377 (2004) 728–732.
[7] Boucharat, et al., Scripta Mater. 53 (7) (2005) 823–828.
[8] A.A. Csontos, G.J. Shiflet, Nanostruct. Mater. 9 (1997) 281–289.
[9] W.H. Jiang, M. Atzmon, Acta Mater. 51 (14) (2003) 4095–4105.
[10] J.-J. Kim, Y. Choi, S. Suresh, A.S. Argon, Science 295 (2002) 654–657.
[11] L.C. Chen, F. Spaepen, Nature 336 (1988) 366–368.
[12] D.R. Allen, J.C. Foley, J.H. Perepezko, Acta Mater. 46 (2) (1998) 431–440.